ATOMS, SPECTRA, RADIATION

Three-Dimensional Interference Effects in the Mechanical Action of Weak Biharmonic Fields upon Particles with the $J = 0 \longrightarrow J = 1$ Quantum Transition

S. A. Gavrilyuk, I. V. Krasnov*, and S. P. Polyutov**

Institute of Computational Modeling, Siberian Division, Russian Academy of Sciences, Krasnoyarsk, 660036 Russia
*e-mail: krasn@ksc.krasn.ru
**e-mail: psp@beep.ru
Received April 23, 2001

Abstract—Explicit expressions are derived for the rectified radiative forces (RRFs) related to the action of a weak interfering optical field of an arbitrary three-dimensional (3D) configuration upon resonance particles featuring the $J = 0 \longrightarrow J = 1$ quantum transition. It is shown that, in contrast to the case of a monochromatic field, there are simple 3D biharmonic field configurations for which the ratio of the vortex and potential RRF components can be controlled by adjusting frequencies and polarizations of the interfering light waves. This modification of the RRF structure gives rise to qualitatively different types of both vortex and potential light-induced particle motions that may lead to a 3D spatial localization (confinement) of these particles within the cells of an effective optical lattice with a period significantly greater than the light wavelength. In particular, the particles may perform a stable rotational motion along closed trajectories inside the elementary cells. © 2001 MAIK "Nauka/Interperiodica".

1. INTRODUCTION

Effective optical control of the motion and spatial localization of resonance atoms [1–3] can be based on the use of the so-called rectified radiative forces (RRFs) [4] induced by interfering biharmonic light fields. This idea was originally formulated in [4–7] and then significantly developed in a number of subsequent theoretical and experimental investigations [8–20]. In a strong field, the RRF possesses a magnitude on the order of an induced light-pressure force, exhibits no saturation with increasing radiation intensity, and has a constant sign over a macroscopic spatial scale significantly exceeding the light wavelength. Another remarkable property of the RRFs, manifested in both strong and weak biharmonic fields, is the possibility of controlling the spatial structure of this force [5, 6, 14, 15]. In a strong biharmonic field, the RRF contains a vortex component besides the potential component, but the ratio of these components can be modified by adjusting the directions of propagation of the interfering waves. This ratio significantly affects the character of the light-induced motion of resonance particles [6, 21, 22]. In the case of a weak biharmonic field, the vortex RRF component can be suppressed, as demonstrated for two-dimensional (2D) field configurations [6], by properly selecting the radiation parameters. This would remove some fundamental limitations (of the type related to the Earnshaw theorem [23]) hindering stable localization of the particles by the forces of spontaneous light pressure in a monochromatic field.

However, these considerations concerning the attractive properties of RRFs were based on the results of calculations performed within the framework of a simple scalar model describing the interaction of an atom with a resonance electromagnetic field. Therefore, strictly speaking, the above conclusions cannot be rigorously transferred to the most interesting case (e.g., for solving the problem of purely optical 3D confinement of atomic species).[1] A correct problem solution requires taking into account degeneracy of the quantum states with respect to the magnetic quantum number M.

Recently, the possibility of ensuring the optical confinement of resonance particles with the aid of RRFs induced by strong fields of a certain 3D configuration was studied by Wasik and Grimm [18] for atoms featuring the quantum transition

$$J_g = 1/2 \longrightarrow J_e = 3/2,$$

where J_g and J_e are the moments of the ground and excited states, respectively.

Degeneracy of the ground state of a resonance particle is a very important feature of the physical situation studied in [18]. This factor predetermines the possibility of existence of a highly successful combination of the effects related to the 3D macroscopic confinement of atoms in a superlattice (induced by a potential RRF), the sub-Doppler (polarization-gradient) cooling, and the microscopic confinement in potential wells with

---

[1] Previous calculations [5, 6] showed only the possibility of an effective 2D localization of particles.

dimensions on the order of a light wavelength. However, a theoretical model proposed in [18] and the theoretical consequences are inapplicable to many atomic species (e.g., such as the alkaline-earth isotopes with even-even nuclei) possessing nondegenerate ground states with $J_g = 0$.

In this study, the theory of interference phenomena in the resonance light pressure is developed for the case of weak bichromatic fields with arbitrary polarizations and 3D spatial configuration and the particles featuring the quantum transition

$$J_g = 0 \longrightarrow J_e = 1.$$

General expressions obtained for the RRFs contain essentially new (in comparison to the scalar model) interference terms related to a nonlinear mixing of the contributions from waves with different frequencies and polarizations to the resonance light pressure. Nevertheless, it was found that the main conclusion made previously about the possibility of controlling the spatial structure of RRFs remains valid. We have established that there exist simple 3D symmetric configurations of the interfering waves (with a zero average total radiation flux density) for which the ratio of the vortex and potential RRF components can be controlled by adjusting frequencies. An additional control factor is provided by polarizations of the interfering light waves which allows, for example, the changing of the axis of rotation for the particles performing a vortex motion in a field with the 3D*Lin* ⊥ *Lin* configuration. Rearrangement of the spatial structure of RRFs is accompanied by the appearance of qualitatively different types of vortex or potential light-induced particle motions that may lead, in particular, to a stable 3D spatial localization of these particles within the cells of an effective macroscopic optical lattice (superlattice) with a period significantly greater than the light wavelength λ.

There is an important circumstance following from the results of our investigation which can be related to the use of weak biharmonic fields for purely optical (nonmagnetic) 3D confinement of atomic species. Even for a relatively small level of saturation of the quantum transition, the RRFs can be still sufficiently large to hold cold particles (with a temperature of $T \sim 10^{-3}$ K corresponding to the Doppler cooling limit in this problem) provided that the field parameters are selected so as to construct a "correct" spatial structure of the RRFs. The advantages of using weak biharmonic fields are (i) a small magnitude of the light-induced Stark shift of the energy levels (not exceeding a natural width γ of the optical resonance), (ii) the possibility of using wide nondiverging laser beams for purely optical confinement of large-size bunches of resonance particles, and (iii) the simplicity of controlling the spatial RRF structure (and, hence, the character of the light-induced motion of particles) without modification of the base geometry of intersecting light rays.

2. A MODEL OF THE ATOM–ELECTROMAGNETIC FIELD INTERACTION

Let us consider an atom possessing the mass m, moving with the velocity **v** in a bichromatic field with the complex amplitude

$$\mathbf{E} = \mathbf{E}_0(\mathbf{r})e^{-i\Delta_0 t} + \mathbf{E}_1(\mathbf{r})e^{-i\Delta_1 t}, \tag{1}$$

where Δ_0 and Δ_1 are the frequency detunings of the fields $\mathbf{E}_0$ and $\mathbf{E}_1$, respectively, from the frequency ω_0 of the quantum transition between the ground state $|J_g = 0, M_g = 0\rangle$ and the excited states $|J_e = 1, M_e = 0, \pm 1\rangle$ of the atom.

The state of this atom in the field will be described in terms of the density matrix $\hat{\rho}$ in a Cartesian representation $\rho_{jj'}^{\beta\beta'}$ [24] using basis functions φ_j^{β} of the type

$$\varphi_0^g = |00\rangle, \quad \varphi_x^e = \frac{|1,-1\rangle - |11\rangle}{\sqrt{2}},$$

$$\varphi_y^e = -i\frac{|1,-1\rangle + |11\rangle}{\sqrt{2}}, \quad \varphi_z^e = |10\rangle.$$

The matrix elements of the operator $\hat{\mathbf{d}}$ of the dipole transition between the atomic states are directed along the axes of the Cartesian coordinate system $\mathbf{e}_j$ ($j = x, y, z$):

$$\langle \varphi_j^e | \hat{\mathbf{d}} | \varphi_0^g \rangle = \mathbf{e}_j d,$$

the amplitude $\mathbf{P}(t)$ of the field-induced atomic dipole moment $\mathrm{Sp}(\rho\hat{\mathbf{d}})$ determined using an expansion

$$\mathbf{p} = \sum_j d\rho_j \mathbf{e}_j,$$

where

$$d = \frac{\langle 1\|d\|0\rangle}{\sqrt{3}},$$

$\langle 1\|d\|0\rangle$ is the reduced matrix element, and

$$\rho_j = \rho_{j0}^{eg}\exp(i\omega_0 t).$$

Exposed to a field of type (1), an atom experiences the action of a force [1]

$$\mathbf{F} = \hbar\sum_j \rho_j \nabla V_j^* + \text{c.c.}, \tag{2}$$

where

$$V_j = \frac{d(\mathbf{e}_j \cdot \mathbf{E})}{\hbar} = \sum_{j\alpha} V_{j\alpha}e^{-i\Delta_\alpha t}, \quad j = x, y, z,$$

$$\alpha = 0, 1, \quad V_{j\alpha}(\mathbf{r}) = \frac{d(\mathbf{e}_j \cdot \mathbf{E}_\alpha(\mathbf{r}))}{\hbar}$$

are the local Rabi frequencies and ρ_j are the projections of the complex amplitude of the induced dipole moment (expressed in units of d) onto the Cartesian coordinate axes. The latter quantities are determined from the optical Bloch equations considered (in the approximation of a preset motion [1]) along the classical atomic trajectory $\mathbf{r} = \mathbf{r}(t)$:

$$i\left(\frac{d}{dt} + \gamma_\perp\right)\rho_i = \sum_j q_{ij} V_j, \quad j, i = x, y, z,$$

$$i\left(\frac{d}{dt} + \gamma\right)q_{ij} = -i\gamma\delta_{ij} + (\rho_i V_j^* - V_i \rho_j^*) \quad (3)$$

$$-\delta_{ij} \sum_{l = x, y, z} (\rho_l^* V_l - \text{c.c.}).$$

Here, we introduced the rate of the spontaneous decay of the excited state $\gamma_\perp = \gamma/2$, and the combinations of elements of the density matrix

$$q_{ij} = \rho_{ij} - \rho\delta_{ij}, \quad \rho_{ij} = \rho_{ij}^{ee},$$

$$\rho = \rho_{00}^{gg} = 1 - (\rho_{xx} + \rho_{yy} + \rho_{zz}).$$

Apparently, ρ has a sense of the relative population of the bottom level, q_{ii} are the differential populations of the working levels, and the quantities q_{ij} ($i \neq j$) describe the effects due to the coherency between states of the excited atom.

We will consider the case of weak fields:[2]

$$\left|\frac{V_{j\alpha}}{v_\alpha}\right|^2, \left|\frac{V_{j\alpha}^2}{v_1 v_2}\right|, \left|\frac{V_{j\alpha}^2}{v_\alpha \gamma}\right| \leq g \ll 1.$$

In this case, the solutions to the Bloch equations and the radiative force can be determined using the perturbation theory. To this end, the unknown quantities are expanded into series in powers of the field strength (in fact, with respect to the small parameter $g \ll 1$):

$$\rho_j = \rho_j^{(1)} + \rho_j^{(3)} + \dots,$$
$$q_{ij} = -\delta_{ij} + q_{ij}^{(2)} + q_{ij}^{(4)} + \dots, \quad (4)$$
$$\mathbf{F} = \mathbf{F}^{(2)} + \mathbf{F}^{(4)} + \dots,$$

where the superscripts indicate the order of smallness.

Nontrivial interference effects in the light-induced pressure appear in the fourth order of smallness with respect to the weak field [5, 6]. For this reason, we

_____

[2] These conditions provide for both a small occupancy of the excited atomic states and a small relative value of the light-induced Stark shift as compared to the resonance width: for $\Delta_\alpha \gg \gamma$, we always have $\left|V_\alpha^2/\gamma\Delta_\alpha\right| \ll 1$. The perturbation theory employed here is inapplicable to the RRF determination, for example, in the case of $|\gamma/\Delta_\alpha|, |V_{j\alpha}/\Delta_\alpha|^2 \ll 1$ if $\left|V_{j\alpha}^2/\gamma\Delta_\alpha\right| \gg 1$ (see [1, 6]).

restrict the expansion of the induced dipole moment ρ_j to terms of the third order. The resulting Bloch equations possess the following structure:

$$\rho_j^{(1)} = \sum_{\alpha=0}^1 A_{j\alpha} e^{-i\Delta_\alpha t},$$

$$\rho_j^{(3)} = \sum_{\alpha=0}^1 A_{j\alpha}^{(3)} e^{-i\Delta_\alpha t} + N_j e^{-i(\delta + \Delta_0)t} + M_j e^{i(\delta - \Delta_1)t}, \quad (5)$$

where $\delta = \Delta_0 - \Delta_1$ ($j = x, y, z$). The functions $A_{\alpha j}$ and $A_{\alpha j}^{(3)}$ are sequentially determined from the following system of linear inhomogeneous equations:

$$\left(\frac{d}{dt} - iv_\alpha\right)A_{j\alpha} = iV_{j0}(\mathbf{r}),$$

$$v_\alpha = \Delta_\alpha + i\gamma_\perp, \quad \mathbf{r} = \mathbf{r}(t),$$

$$\left(\frac{d}{dt} - iv_0\right)A_{i0}^{(3)} = -i\sum_j (C_{ij} V_{j0}(\mathbf{r}) + D_{ij} V_{j1}(\mathbf{r})),$$

$$v_{01} = \delta + i\gamma,$$

$$\left(\frac{d}{dt} - iv_1\right)A_{i1}^{(3)} = -i\sum_j (C_{ij} V_{j1}(\mathbf{r}) + D_{ji}^* V_{j0}(\mathbf{r})), \quad (6)$$

$$\left(\frac{d}{dt} + \gamma\right)C_{ij} = i\sum_\alpha (A_{j\alpha}^* V_{i\alpha}(\mathbf{r}) - A_{i\alpha} V_{j\alpha}^*(\mathbf{r}))$$

$$-i\delta_{ij} \sum_{l,\alpha} (A_{l\alpha} V_{l\alpha}^*(\mathbf{r}) - \text{c.c.}),$$

$$\left(\frac{d}{dt} - iv_{01}\right)D_{ij} = i(V_{i0}(\mathbf{r}) A_{j1}^* - V_{j1}(\mathbf{r}) A_{i0})$$

$$+i\delta_{ij} \sum_l (V_{l0}(\mathbf{r}) A_{l1}^* + V_{l1}^*(\mathbf{r}) A_{l0}).$$

In what follows, we will assume that the frequency detunings Δ_0 and Δ_1 are not very close to each other ($|\Delta_0 - \Delta_1| > g\gamma$). This allows us to write an expression for the force with neglect of the terms oscillating at the frequencies representing the multiples of $\delta = \Delta_0 - \Delta_1$.[3] It is also not necessary to determine explicitly the components $\rho_j^{(3)} \propto M_j$ and N_j.

_____

[3] An allowance for these terms leads to small (in the quasi-classical limit of $mv \gg \hbar\omega_0/c$) oscillating corrections $\delta p < \hbar\omega_0/c$ to the particle momentum [5].

3. RECTIFIED RADIATION FORCES

As can be readily seen from the above Eqs. (2) and (4)–(6), the interfering light fields are of the plane wave superposition type with the wave vectors $\{\mathbf{k}_\alpha^\sigma\}$:

$$\mathbf{E}_\alpha(\mathbf{r}) = \sum_\sigma \mathbf{E}_\alpha^\sigma \exp(i\mathbf{k}_\alpha^\sigma \cdot \mathbf{r}), \qquad (7)$$

in which the radiative force is a nonlinear function of both the wave amplitude $\left|\mathbf{E}_\alpha^\sigma\right|$ and the ratios of phases and polarizations; in other words, the field dependence of the force exhibits a pronounced interference character.

Let us assume that the sets of wavevectors $\{\mathbf{k}_0^\sigma\}$, $\{\mathbf{k}_1^\sigma\}$ contain the pairs $\mathbf{k}_\alpha^\sigma$, $\mathbf{k}_{\alpha'}^{\sigma'}$ such that

$$\left|\mathbf{k}_\alpha^\sigma - \mathbf{k}_{\alpha'}^{\sigma'}\right| \sim \Delta k \ll k.$$

In this case, a quasi-periodic spatial structure of the force is characterized by two sharply different scales: microscopic (on the order of the light wavelength $\lambda \sim 1/k$) and macroscopic ($\lambda_M \sim \Delta k^{-1} \gg \lambda$) related to beats of the spatial harmonics with close wavevectors $\mathbf{k}_\alpha^\sigma$.

The rectified radiative force [5, 6] is a smooth component of the radiative force $\langle \mathbf{F} \rangle$ averaged over the microscopic spatial oscillations. Note that the spatial variation of this force is determined by the macroscopic quantity λ_M, while the characteristic magnitude is determined on the microscopic (!) scale:[4]

$$|\langle \mathbf{F} \rangle| \propto k \sim 1/\lambda.$$

We will restrict the consideration to the case of slow atoms (frequently encountered in modern experiments),

$$kv \ll \gamma, \qquad (8)$$

and take into account the nonlocal (retarding) part of the field-induced dipole moment in solving Eq. (6) in the linear approximation with respect to the velocity. Under these conditions, Eqs. (2) and (4)–(6) give the following expressions for the RRF (to within the terms on the order of $\sim g^2$):

$$\langle \mathbf{F} \rangle = \mathbf{F}_{0R} + \mathbf{F}_{1R} + \mathbf{F}_R. \qquad (9)$$

Here, $\mathbf{F}_{0R}$ and $\mathbf{F}_{1R}$ are the RRF components of the second order in the field amplitude, representing the sums of independent contributions of the $\mathbf{E}_0$ and $\mathbf{E}_1$ fields,

$$\mathbf{F}_{0R} = \hbar\gamma \sum_{\alpha, j} \frac{\langle \mathbf{J}_{j\alpha} \rangle}{|\nu_\alpha|^2}, \qquad (10)$$

$$\mathbf{J}_{j\alpha} = \frac{i}{2}(V_{j\alpha}\nabla V_{j\alpha}^* - \text{c.c.}), \quad j = x, y, z,$$

$$\mathbf{F}_{1R} = \hbar\gamma \sum_{\alpha, j} \frac{\Delta_\alpha}{|\nu_\alpha|^4} \langle (\mathbf{v} \cdot \nabla V_{j\alpha})\nabla V_{j\alpha}^* + \text{c.c.} \rangle$$

$$- \hbar i \sum_{\alpha, j} \frac{\Delta_\alpha^2 - \gamma_\perp^2}{|\nu_\alpha|^4} \langle [\mathbf{v} \times [\nabla V_{j\alpha} \times \nabla V_{j\alpha}^*]] \rangle, \qquad (11)$$

and $\mathbf{F}_R$ is the RRF component of the fourth order in the field amplitude:

$$\mathbf{F}_R = -2\hbar\gamma \sum_\alpha \frac{\langle \mathbf{J}_\alpha I_\alpha \rangle}{|\nu_\alpha|^4} + \frac{\hbar}{|\nu_0|^2 |\nu_1|^2}\left\{ \Lambda \left[\langle I_0 \nabla I_1 \rangle \right.\right.$$

$$\left. + \sum_j \langle I_{j0} \nabla I_{j1} \rangle + \frac{1}{2}\sum_{j \neq l}(\langle I_0^{lj} \nabla I_1^{jl} \rangle + \text{c.c.}) \right]$$

$$- \Lambda_1 \left[\langle I_0 \mathbf{J}_1 \rangle + \sum_j \langle \mathbf{J}_{j0} I_{j1} \rangle + \frac{1}{2}\sum_{j \neq l}(\langle \mathbf{J}_0^{jl} I_1^{jl} \rangle + \text{c.c.}) \right]$$

$$\left. - \Lambda_0 \left[\langle I_1 \mathbf{J}_0 \rangle + \sum_j \langle \mathbf{J}_{j1} I_{j0} \rangle + \frac{1}{2}\sum_{j \neq l}(\langle \mathbf{J}_1^{jl} I_0^{lj} \rangle + \text{c.c.}) \right] \right\}, \qquad (12)$$

$$\mathbf{J}_\alpha = \sum_j \mathbf{J}_{j\alpha},$$

$$\mathbf{J}_\alpha^{jl} = \frac{i}{2}(V_{l\alpha}\nabla V_{j\alpha}^* - V_{j\alpha}^*\nabla V_{l\alpha}), \quad \mathbf{J}_{j\alpha} = \mathbf{J}_\alpha^{jj},$$

$$I_\alpha = \sum_j I_{j\alpha}, \quad I_{j\alpha} = |V_{j\alpha}|^2,$$

$$I_\alpha^{jl} = V_{j\alpha}^* V_{l\alpha}, \quad j, l = x, y, z,$$

$$\Lambda = [(\Delta_1 - \Delta_0)(1 - \cos\chi) - \gamma\sin\chi],$$

$$\Lambda_1 = [\gamma(1 + \cos\chi) - 2\Delta_1\sin\chi],$$

$$\Lambda_0 = [\gamma(1 + \cos\chi) + 2\Delta_0\sin\chi],$$

$$\nu_\alpha = |\nu_\alpha|\exp(i\chi_\alpha), \quad \chi = 2(\chi_1 - \chi_0), \qquad (13)$$

where angular brackets denote averaging over the microscopic spatial oscillations.

It should be noted that the quantities $I_{j\alpha}(\mathbf{r})$ and $\mathbf{J}_{j\alpha}(\mathbf{r})$ are proportional, respectively, to the "intensity" (square modulus of the complex amplitude) and the energy flux density of the field components (polarized in the direction of the unit vector $\mathbf{e}_j$ and belonging to the same αth mode) in the superposition (7). The supplementary

---

[4] In other words, the RRF exists provided that the averaging procedure does not reduce the force magnitude $|\langle \mathbf{F} \rangle| \sim |\mathbf{F}| \propto k$ in the order of magnitude (with respect to the parameter $\lambda/\lambda_M \ll 1$) [5].

quantities I_α^{jl} and $\mathbf{J}_\alpha^{jl}$ with $j \neq l$ represent a measure of "mixing" of the waves with different polarizations belonging to the same mode (indeed, $I_\alpha^{jl}, J_\alpha^{jl} = 0$ provided that at least one of the amplitudes $|V_{j\alpha}|$ or $|V_{l\alpha}|$ is zero). In a particular case of the 2D field configuration, when all waves in the superposition (7) are polarized along one of the Cartesian axes $\mathbf{e}_z$ (i.e., $\mathbf{E}_\alpha^\sigma \propto \mathbf{e}_z$), we obtain $J_\alpha^{jl} = I_\alpha^{jl} = 0$ for $j \neq l$ and $I_{j\alpha} \propto J_{j\alpha} \propto \delta_{zj}$, so that expressions (12) convert into relationships (25) derived in [5].

Essentially new interference terms in expression (12), which are due to the polarization effects, are related to correlators of the intensity–flux type ($\langle \mathbf{J}_{j\alpha}, I_{l\alpha} \rangle, j \neq l$) referring to the waves of different polarizations with the same frequencies (intramode interference) and correlators of the intensity–flux and intensity–intensity types ($\langle \mathbf{J}_{j\alpha'}, I_{l\alpha} \rangle, \langle I_{j\alpha} \nabla I_{l\alpha} \rangle, j \neq l, \alpha \neq \alpha'$) referring to the waves of different polarizations and different frequencies (intermode interference). The intermode interference is also determined by the correlators involving mixed products of the projections of the complex field amplitudes and their derivatives of the types $\langle \mathbf{J}_\alpha^{jl} I_{\alpha'}^{lj} \rangle$ and $\langle I_\alpha^{jl} \nabla I_{\alpha'}^{lj} \rangle$, where $\alpha \neq \alpha'$ and $j \neq l$.

One of the most important factors determining the light-induced motion of resonance particles is the character of the spatial RRF structure. It should be kept in mind that, under the conditions studied, the principal part of the RRF expansion into perturbative series (i.e., the $\mathbf{F}_{0R}$ force component) always possesses a purely vortex structure. Indeed, calculation of the average radiation flux densities $\langle \mathbf{J}_\alpha \rangle$ in the case of field superpositions of the type (7) yields

$$\langle \mathbf{J}_{j\alpha} \rangle = \sum_\sigma \mathbf{k}_\alpha^\sigma |a_{j\alpha}^\sigma|^2 + \frac{1}{2}$$

$$\times \left[\sum_{\eta > \gamma} (\mathbf{k}_\alpha^\eta + \mathbf{k}_\alpha^\gamma)(a_{j\alpha}^\eta)^* a_{j\alpha}^\gamma \exp[i(\phi_\alpha^\gamma - \phi_\alpha^\eta)] + \text{c.c.} \right],$$ (14)

where

$$\phi_\alpha^\gamma = \mathbf{k}_\alpha^\gamma \cdot \mathbf{r}, \quad a_{j\alpha}^\gamma = \mathbf{e}_j \cdot \mathbf{E}_\alpha^\gamma.$$

In the double sum, the indices γ, η refer to all possible pairs of wavevectors with close orientations:

$$|\mathbf{k}_\alpha^\gamma - \mathbf{k}_\alpha^\sigma| \ll k.$$

Expressions (14) and (10) are clearly indicative of the vortex character of the $\mathbf{F}_{0R}$ force component, since

$$\text{div} \mathbf{F}_{0R} = 0.$$

Note that this is essentially an expression of the Earnshaw theorem [23] for the RRF. Such a "defect" in the spatial RRF structure formed in a weak monochromatic field ($\mathbf{E}_1 = 0$) is basically inavoidable. Indeed, although a correction $\mathbf{F}_R$ to the rectified radiative force in the fourth order of smallness with respect to the field amplitude contains both vortex and potential components, the ratio of the former to the latter is fixed and cannot be changed arbitrarily by modifying the field parameters and configurations [6]. This circumstance significantly limits the possibility of using weak monochromatic fields for controlling the motion and spatial localization of resonance particles. An essentially different physical situation is observed in the case of bichromatic fields, provided that the total radiation flux densities for each frequency mode turn zero,

$$\sum_j \langle \mathbf{J}_{j\alpha} \rangle = 0, \quad j = x, y, z,$$ (15)

which implies that the principal vortex component of the RRF is suppressed ($\mathbf{F}_{0R} = 0$).

Now we will consider three examples of particular 3D field configurations satisfying conditions (15). In these examples, $\mathbf{F}_{1R}$ is the friction force and the $\mathbf{F}_R$ exhibits either a purely potential or potential–vortex character with a fully controllable ratio of the vortex and potential components.

3.1. Mutually Orthogonal Standing Waves

Let us consider mutually orthogonal standing waves (Fig. 1a):

$$V_{x\alpha} = V_\alpha \cos(k_\alpha z), \quad V_{y\alpha} = V_\alpha \cos(k_\alpha x),$$
$$V_{z\alpha} = V_\alpha \cos(k_\alpha y).$$ (16)

Upon substituting (16) into Eqs. (10)–(12), we obtain

$$\mathbf{F}_{1R} = -m\kappa\mathbf{v}, \quad \kappa = -\frac{\hbar k^2 \gamma}{m} \left(\frac{V_0^2 \Delta_0}{|\nu_0|^4} + \frac{V_1^2 \Delta_1}{|\nu_1|^4} \right),$$ (17)

$$\mathbf{F}_R = -\nabla U(\mathbf{r}),$$

$$U(\mathbf{r}) = -\frac{\hbar \Gamma_1 k V_1^2 V_0^2}{4\delta k |\nu_1|^2 |\nu_0|^2} \left\{ \sum_j \cos(2\delta k \mathbf{e}_j \cdot \mathbf{r}) \right.$$

$$\left. + \frac{1}{2} \sum_{i \neq j} (\cos[\delta k(\mathbf{e}_i - \mathbf{e}_j) \cdot \mathbf{r}] + \cos[\delta k(\mathbf{e}_i + \mathbf{e}_j) \cdot \mathbf{r}]) \right\},$$

where

$$\delta k = k_1 - k_0 = \frac{\Delta_1 - \Delta_0}{c},$$

m is the particle mass, and Γ_1 is a function of the relaxation constants and frequency detunings:

$$\Gamma_1 = \gamma\gamma_\perp (\Delta_1 - \Delta_0) \left(\frac{1}{|\nu_1|^2} + \frac{1}{|\nu_0|^2} \right).$$
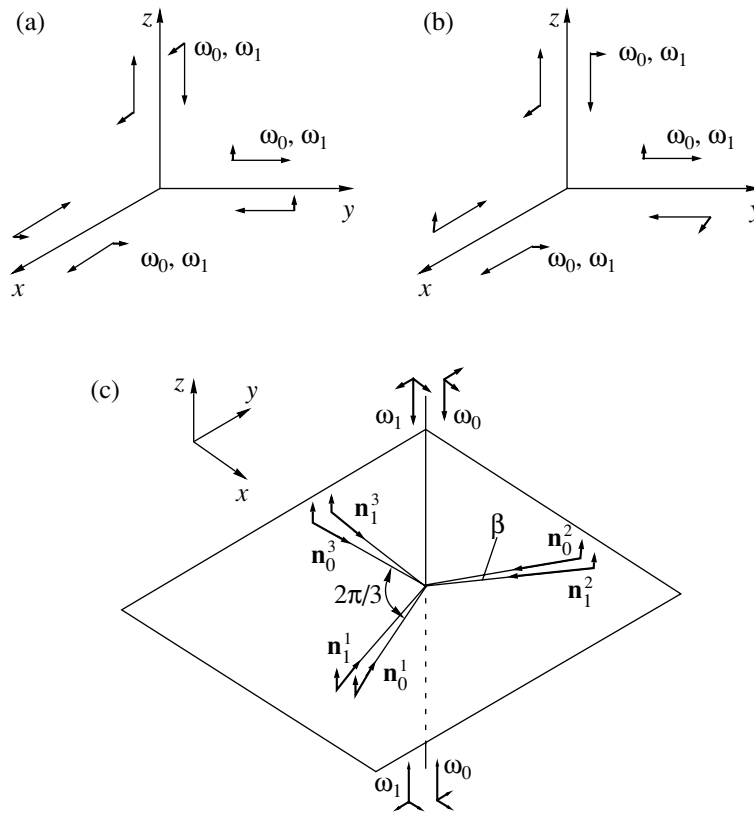
Fig. 1. Three-dimensional optical field configurations satisfying conditions (15): (a) a superposition of mutually orthogonal standing waves; (b) 3D*Lin* ⊥ *Lin* field configuration; (c) a superposition of standing (along the *z* axis) and linearly polarized (in the same direction) traveling waves. Long arrows show the directions of wave propagation; short arrows indicate polarizations of the interfering waves; ω_α is the wave frequency, $\mathbf{n}_\alpha^\sigma$ are the unit vectors in the propagation directions of waves with frequencies ω_α; $\beta \ll 1$ is the angular deviation.

Thus, $\mathbf{F}_{1R}$ is a friction force (for $\kappa(\Delta_1, \Delta_0) > 0$), while the rectified radiative force $\mathbf{F}_R$ exhibits a purely potential character. In the vicinity of the RRF nodes $\mathbf{r}_0$ corresponding to the point of minima for the $U(\mathbf{r})$ function,

$$\mathbf{r}_0 = \frac{\pi}{\delta k}(m\mathbf{e}_x + [m + 2n]\mathbf{e}_y + [m + 2p]\mathbf{e}_z), \quad (18)$$

the potential has a spherically symmetric character. For $2\delta kR < 1$, this potential can be presented in the following form:

$$U(\mathbf{r}) \approx \frac{1}{2}U_0\delta k^2 R^2,$$

$$U_0 = \hbar\omega_0\left(\frac{\gamma^2}{|\nu_1|^2} + \frac{\gamma^2}{|\nu_0|^2}\right)\frac{V_1^2 V_0^2}{|\nu_1|^2|\nu_0|^2}, \quad (19)$$

where $m, n, p \in Z$ (Z is the set of integers) and $R = |\mathbf{r} - \mathbf{r}_0|$ is the displacement from the RRF node; in writing (19), an insignificant constant additive was omitted.

It should be noted that the RRF nodes of the $\mathbf{r}_0$ type form a body-centered-cubic (bcc) lattice, the period of

which ($\pi/\delta k$) can be controlled by varying the field detunings.

3.2. A Lin ⊥ Lin Wave Superposition (3D Lin ⊥ Lin Configuration)

Let us consider a superposition of waves with *Lin* ⊥ *Lin* configuration:

$$V_{x\alpha} = V_\alpha(e^{ik_\alpha z} + e^{-ik_\alpha y}),$$

$$V_{y\alpha} = V_\alpha(e^{ik_\alpha x} + e^{-ik_\alpha z}), \quad (20)$$

$$V_{z\alpha} = V_\alpha(e^{ik_\alpha y} + e^{-ik_\alpha x}).$$

In this superposition, each wave propagating along one of the three Cartesian coordinate axes is supplemented with an opposite wave (counterwave) of the same frequency, polarized in the perpendicular direction (Fig. 1b). In comparison with the configuration depicted in Fig. 1a, only the polarization direction of one wave in each pair is changed. However, a spatial structure of the RRF exhibits a significant qualitative variation, which can be considered as a manifestation

of the polarization effects in the resonance light-induced pressure.

Indeed, the friction coefficient κ_1 and the RRF component $\mathbf{F}_R$ in this case are described by the following expressions:

$$\kappa_1 = 4\kappa, \quad \mathbf{F}_R = -\nabla U + \mathrm{rot}\mathbf{A}, \tag{21}$$

where κ is a coefficient determined by formula (17). The scalar (U) and vector ($\mathbf{A}$) RRF potentials introduced in (21) can be expressed as follows:

$$\mathbf{A} = A_0\Psi(\mathbf{r})\mathbf{e}, \quad \mathbf{e} = \frac{1}{\sqrt{3}}(\mathbf{e}_x + \mathbf{e}_y + \mathbf{e}_z),$$

$$A_0 = \frac{2\sqrt{3}\hbar k V_0^2 V_1^2 \Gamma}{|v_0|^2 |v_1|^2 \delta k},$$

$$\Psi(\mathbf{r}) = \sin[\delta k(y+z)] + \sin[\delta k(x+z)]$$
$$+ \sin[\delta k(x+y)],$$

$$\Gamma = \gamma(1 + \cos\chi) + (\Delta_0 - \Delta_1)\sin\chi \tag{22}$$

$$= (\Delta_1\Delta_0 + \gamma_\perp^2)\left(\frac{\gamma}{|v_0|^2} + \frac{\gamma}{|v_1|^2}\right),$$

$$U = -U_0\left(\sum_j \cos(2\delta k\mathbf{e}_j \cdot \mathbf{r})\right.$$

$$+ \frac{1}{2}\sum_{i \neq j}(3\cos[\delta k(\mathbf{e}_i + \mathbf{e}_j)\cdot\mathbf{r}] + 2\cos[\delta k(\mathbf{e}_i - \mathbf{e}_j)\cdot\mathbf{r}]) \bigg),$$

$$U_0 = -\tan\left(\frac{\chi}{2}\right)A_0 = \hbar\omega_0\left(\frac{\gamma^2}{|v_1|^2} + \frac{\gamma^2}{|v_0|^2}\right)\frac{V_1^2 V_0^2}{|v_0|^2 |v_1|^2}.$$

It is seen that the RRF represents a combination of the potential force and the vortex component

$$\mathbf{F}_{\mathrm{vort}} = \mathrm{rot}\mathbf{A}.$$

The ratio of the two components is proportional to

$$\tan\left(\frac{\chi}{2}\right) = \gamma_\perp\frac{\Delta_0 - \Delta_1}{\Delta_1\Delta_0 + \gamma_\perp^2}$$

and can be controlled (virtually arbitrarily) by adjusting the field frequencies. Indeed, for

$$\Delta_1\Delta_0 = -\gamma_\perp^2$$

the RRF is purely potential, while for

$$\Delta_1\Delta_0 \sim -\gamma_\perp^2 \quad \left(\left|\tan\left(\frac{\chi}{2}\right)\right| \gg 1\right),$$

a small vortex "admixture" appears in the still dominating potential component, and for

$$\left|\tan\left(\frac{\chi}{2}\right)\right| \ll 1 \quad \left(\gamma g < |\Delta_0 - \Delta_1| \ll \left|\gamma_\perp + \frac{\Delta_0\Delta_1}{\gamma_\perp}\right|\right)$$

the vortex component begins to prevail and the potential component becomes a small admixture.

The positions of the RRF nodes $\mathbf{r}_0$ in which the potential function exhibits absolute minima is determined (as well as in the preceding example) by formula (18). However, the potential in a small vicinity of these nodes is no longer spherically symmetric. In a small region near $\mathbf{r}_0$, such that $2\delta kr < 1$, the potential can be expressed as

$$U(r) \approx \frac{U_0}{2}(16\eta + 13[\xi^2 + \zeta^2]) + \mathrm{const},$$

$$\eta = \frac{\delta k(x+y+z)}{\sqrt{3}}, \quad \xi = \frac{\delta k(2z-x-y)}{\sqrt{6}},$$

$$\zeta = \frac{\delta k(x-y)}{\sqrt{2}}.$$

According to this, the potential level surfaces at the nodes $\mathbf{r}_0$ possess the shape of an ellipsoid of revolution with an axis parallel to the bisector of the first octant of the Cartesian coordinate system—the straight line C determined by the equation

$$\mathbf{r} = \mathbf{r}(\sigma) = \sigma\mathbf{e}, \quad -\infty < \sigma < \infty.$$

This circumstance is directly related to the symmetry of the optical field, since the line C is a third-order symmetry axis for the 3D*Lin* $\perp$ *Lin* field configuration: rotation of all wave vectors and polarization vectors about this axis by an angle of $2\pi/3$ leaves the initial configuration unchanged. The presence of the symmetry axis C also determines to a considerable extent the structure of the vortex field $\mathbf{F}_{\mathrm{vort}}$. Indeed, according to expressions (21) and (22),

$$\mathbf{F}_{\mathrm{vort}} \cdot \mathbf{e} = 0,$$

which implies that the vector field lines of the vortex RRF component are lying in the Π_c planes (determined by the equations $\mathbf{r} \cdot \mathbf{e} = c$) perpendicular to the symmetry axis $\mathbf{e}$. The set of periodically arranged lines

$$\mathbf{r} = \mathbf{r}(\sigma, \mathbf{r}_0) = \mathbf{r}_0 + \sigma\mathbf{e},$$

parallel to the axis C represents the nodal lines for the vortex RRF force component: $\mathbf{F}_{\mathrm{vort}}(\mathbf{r}(\sigma, \mathbf{r}_0)) = 0$. In addition, taking into account that

$$\nabla\Psi \cdot \mathbf{F}_{\mathrm{vort}} = 0,$$

we infer that the vector lines of the vortex force field represent the curves of intersection of the level planes Π_c with the level surfaces of the function $\Psi(\mathbf{r})$. In a small vicinity of the nodal lines $\mathbf{r} = \mathbf{r}(\sigma, \mathbf{r}_0)$, these curves appear as circumferences in the Π_c plane with

the centers occurring at the points of intersection of the planes Π_c and the nodal lines $\mathbf{r} = \mathbf{r}(\sigma, \mathbf{r}_0)$. As is demonstrated below, the resonance particles can perform the light-induced rotational motions about these centers (see the next Section).

The symmetry axis C in the 3D$Lin \perp Lin$ configuration (and, hence, the "particle rotation axes") can be readily changed by consistently changing the wave polarizations. For example, the direction of this axis in a field of the 3D$Lin \perp Lin$ configuration is determined by the formulas

$$V_{x\alpha} = V(\exp(-ik_\alpha z) + \exp(-ik_\alpha y)),$$
$$V_{y\alpha} = V(\exp(ik_\alpha x) + \exp(ik_\alpha z)),$$
$$V_{z\alpha} = -V(\exp(-ik_\alpha x) + \exp(ik_\alpha y)),$$

and represented by the vector

$$\mathbf{e}_1 = \frac{\mathbf{e}_x + \mathbf{e}_y - \mathbf{e}_z}{\sqrt{3}}.$$

3.3. A Superposition of Standing and Linearly Polarized Traveling Waves

Let us consider a superposition of standing (along the z axis) and linearly polarized (in the same direction) traveling waves with a symmetric triangular configuration, intersecting in the xy plane (Fig. 1c):

$$V_{x1} = \hat{V}_1 \cos[(k + \delta k)z],$$
$$V_{y1} = -\hat{V}_1 \cos[(k + \delta k)z],$$
$$V_{j0} = \hat{V}_0 \cos kz, \quad j = x, y, \tag{23}$$
$$V_{z\alpha}(\mathbf{r}) = V_\alpha \sum_{\sigma=1}^{3} \exp[i\hat{\varphi}_\alpha^\sigma(\mathbf{r})],$$

where

$$\hat{\varphi}_0^\sigma(\mathbf{r}) = k\mathbf{n}_0^\sigma \cdot \mathbf{r} + \varphi_0^\sigma,$$
$$\hat{\varphi}_1^\sigma(\mathbf{r}) = (k + \delta k)\mathbf{n}_1^\sigma \cdot \mathbf{r} + \varphi_1^\sigma, \quad k = k_0,$$

the unit vectors determining the directions of wavevectors $\mathbf{n}_\alpha^\sigma$ are lying in the xy plane,

$$\mathbf{n}_0^\sigma = (\cos(2\pi\sigma/3), \sin(2\pi\sigma/3), 0), \quad \sigma = 1, 2, 3,$$

and the system of vectors $\mathbf{n}_1^\sigma$ is "rigidly" rotated about the z axis relative to $\mathbf{n}_0^\sigma$ vectors by a small angle $\beta \ll 1$. Assuming that

$$\delta k/k \ll \beta \ll 1,$$

restricting the consideration to a region

$$\rho = \sqrt{x^2 + y^2} < 1/\delta k,$$

and using Eqs. (10)–(12) and (23), we obtain the following expressions:

$$\mathbf{F}_{1R} = -m(\kappa_\perp \mathbf{v}_\perp + \kappa_z \mathbf{e}_z v_z),$$

$$\kappa_\perp = -\frac{3\hbar k^2}{m}\gamma\left(\frac{V_1^2 \Delta_1}{|\nu_1|^4} + \frac{V_0^2 \Delta_0}{|\nu_0|^2}\right),$$

$$\kappa_z = -\frac{2\hbar k^2}{m}\gamma\left(\frac{\hat{V}_1^2 \Delta_1}{|\nu_1|^4} + \frac{\hat{V}_0^2 \Delta_0}{|\nu_0|^2}\right),$$

$$\mathbf{F}_R = -\frac{2\hbar\Gamma}{|\nu_0|^2 |\nu_1|^2}\left\{\frac{V_1^2 V_0^2}{\beta}\right. \tag{24}$$

$$\times \left[\nabla U(\mathbf{r}) + \tan\left(\frac{\chi}{2}\right)\text{rot}\,\mathbf{a}(\mathbf{r})\right]$$

$$\left. + \tan\left(\frac{\chi}{2}\right)\frac{\hat{V}_1^2 \hat{V}_0^2}{4\delta k}\mathbf{e}_z\frac{\partial U_1(z)}{\partial z}\right\},$$

where

$$\mathbf{v}_\perp = \mathbf{e}_x v_x + \mathbf{e}_y v_y, \quad U_1(z) = 2\cos(2\delta kz),$$

$$\mathbf{a}(\mathbf{r}) = 2\Psi_1(\mathbf{r})\mathbf{e}_z,$$

$$\Psi_1(\mathbf{r}) = \sum_{\sigma=1}^{3}\cos(\beta\sqrt{3}k\mathbf{n}_0^\sigma \cdot \mathbf{r} + \xi_\sigma),$$

$$U(\mathbf{r}) = -\frac{2}{\sqrt{3}}\sum_{\sigma=1}^{3}\sin(\beta\sqrt{3}k\mathbf{n}_0^\sigma \cdot \mathbf{r} + \xi_\sigma),$$

$$\xi_1 = [\varphi_0^2 - \varphi_1^2] - [\varphi_0^3 - \varphi_1^3],$$

and the constant phases ξ_2 and ξ_3 are obtained from ξ_1 by the cyclic permutation of indices. In this force field, the motions in the xy plane and along the z axis are completely separated and independent. A force acting along the z axis is always potential and possesses a periodic spatial structure with the period $\pi/\delta k$. A ratio of the vortex and potential force components acting in the directions parallel to the xy plane is proportional to $\tan(\chi/2)$ and, hence, can be fully controlled by selecting appropriate field frequency detunings Δ_1 and Δ_0 Here, both potential and vortex RRF components possess a periodic spatial structure.

Figure 2 shows the pattern of level lines for the potential function $U(x, y)$. The point of intersection of the separatrix lines represent the saddle points forming a planar hexagonal lattice with the period

$$\lambda_M = 4\pi/3k\beta,$$

determined by the angular deviation β. Located at the centers of the triangular separatrix cells are the points of minima (denoted by dots in Fig. 2) and maxima of
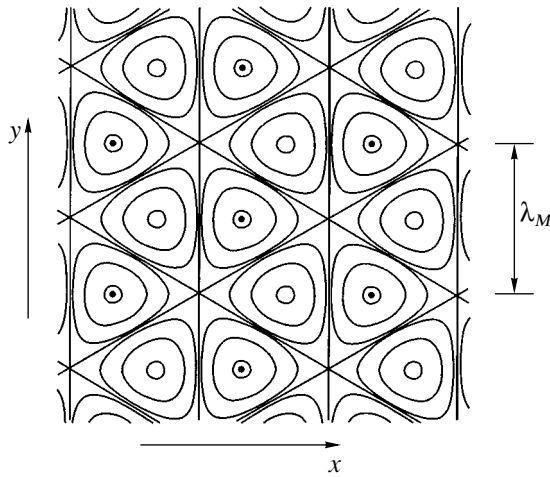
Fig. 2. A schematic diagram showing the level lines of the potential function $U(r)$ described by Eq. (24) determining the potential RRF component in a field configuration of the third type, acting in the directions parallel to the xy plane. Dots at the centers of some cells indicate the points of minima of the function $U(r)$; $\lambda_M = 4\pi/3k\beta$ is the macroscopic spatial scale.

4. FEATURES OF THE LIGHT-INDUCED MOTION OF PARTICLES

Let b denote the characteristic size of a region featuring intersection of real laser beams and containing resonance particles. The interference effects in the light-induced motion of the resonance particles can be fully manifested provided that the macroscopic spatial scale λ_M (in the field model under consideration, this value corresponds to the period of an optical superlattice formed as a result of the superposition of plane waves (7)) does not exceed b:

$$\lambda_M < b.$$

Taking into account that

$$\lambda_M \sim \frac{1}{|\delta k|} = \frac{c}{|\Delta_1 - \Delta_0|},$$

and a typical value of the spontaneous relaxation rate is $\gamma \sim 10^8 \text{ s}^{-1}$, this condition can be fulfilled even for wide beams ($b \sim 10\text{–}20$ cm) if the field frequency difference is significantly greater than the resonance width:

$$|\Delta_1 - \Delta_0| \gg \gamma.$$

With an allowance for this circumstance, an optimum set of the field frequencies and amplitudes (selected based on the criterion of maximum RRF at a fixed value of the parameter g) must obey the following relationships:

$$|v_0| \sim \gamma, \quad |\Delta_1| \gg \gamma, \quad \left|V_{j1}^2/v_1 v_0\right| \sim \left|V_{j0}/v_0\right|^2 \sim g \ll 1,$$

$$\left|V_{j1}/v_1\right|^2 \ll g.$$

For $\Delta_0 < 0$, the field $\mathbf{E}_0$ is responsible for the cooling process and the field $\mathbf{E}_1$ (together with $\mathbf{E}_0$), for the man-

the function $U(x, y)$. The extremal points of both types also form mutually shifted planar hexagonal lattices.

Figure 3 shows the vector field lines of the vortex RRF component. Here, the network of the separatrix lines (described by the equation $\Psi_1(\mathbf{r}) = -1$) forms the so-called kagome lattice. Vector lines inside the triangular and hexagonal cells of this lattice represent closed curves surrounding special points (centers) coinciding with the positions of saddle point (in the hexagonal cells) and extremal points (in the triangular cells) of the potential function $U(x, y)$.
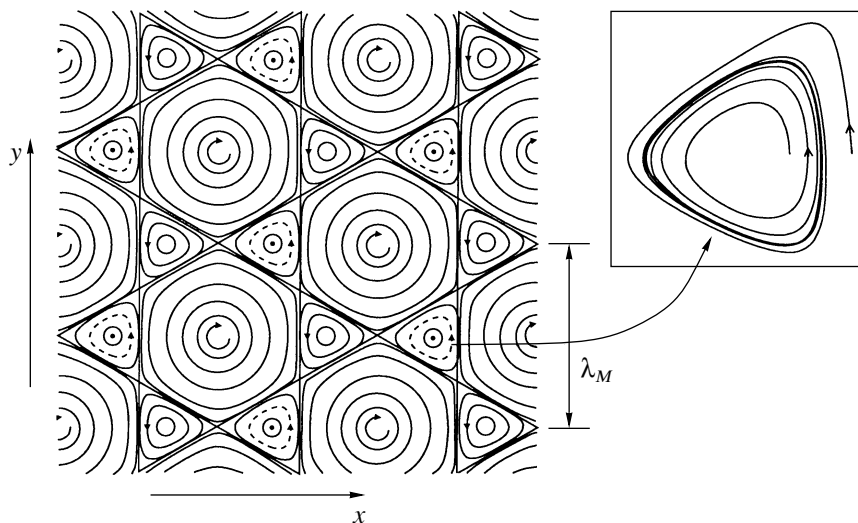

Fig. 3. A schematic diagram of the kagome lattice formed by vector lines of a vortex RRF component induced by interfering optical fields with a configuration of the third type. Dashed lines show stable closed particle trajectories (limiting cycles), which may appear only in the triangular cells containing the points of minima of the potential function $U(\mathbf{r})$. The inset shows a typical trajectory of a particle falling within the separatrix lattice cell.

ifestation of interference effects. The characteristic values of the friction coefficient and the RRF can be estimated from the following simple relationships:

$$\kappa = \omega_r g, \quad \omega_R = \frac{\hbar k^2}{m}, \quad |\mathbf{F}_R| = F \sim \hbar k \gamma g^2.$$

The RRF component $\mathbf{F}_R$ will be the main factor determining (together with the friction force) the light-induced motion of an ensemble of resonance particles with the temperature T (expressed in the energy units) under the following conditions:

$$U_g \ll T \ll \Delta U, \tag{25}$$

where U_g is the depth of microscopic potential wells formed under the action of rapidly oscillating (with a period $\sim\lambda$) gradient forces [1, 2], $\Delta U \sim F\lambda_M$ is the characteristic work performed by the RRF for the transfer of particles over a macroscopic distance λ_M (for the potential RRFs, ΔU is the depth of macroscopic potential wells). The temperature T corresponding to the so-called Doppler cooling limit is established within a characteristic time $\sim\kappa^{-1}$ as a result of the competition between the Doppler cooling and the diffusion processes in the velocity space [1, 2] determined by the quantum fluctuations of radiative forces.

For a selected ratio of the main problem parameters, the rate of the velocity diffusion is [1, 2]

$$D \sim \left(\frac{\hbar k}{m}\right)^2 \gamma g, \quad T \sim \frac{mD}{\kappa} \sim \hbar \gamma, \quad U_g \sim \hbar \gamma g.$$

For $g \ll 1$, the left-hand inequality in (25) is always fulfilled, which implies impossibility of confining particles at the small-scale potential wells. The right-hand inequality (25) indicates that the field must not be very weak:

$$1 \gg g^2 > 1/k\lambda_M.$$

An important feature of the light-induced motion of particles in a weak bichromatic field for $\kappa > 0$ is the overdamped character of this motion which is caused by a large friction force:

$$\frac{\Omega^2}{\kappa^2} = \varepsilon \sim \frac{\gamma}{\omega_R} \frac{\Delta k}{k} \ll 1, \tag{26}$$

where $\Omega = \sqrt{F\Delta k/m}$ is the characteristic frequency of motion in the absence of friction; $\Delta k = |\delta k|$ for a field configuration of the first or second type and $\Delta k = k|\beta|$, for the third type (see the preceding section). The smallness of the parameter ε is related to smallness of the ratio of the microscopic and macroscopic scales. Indeed, for the typical values of $\gamma/\omega_R \sim 10^2$–$10^3$, $k = 10^5$ cm^{-1}, and $\Delta k \sim 1$ cm^{-1}, relationship (26) yields an estimate $\varepsilon \sim 10^{-2}$–10^{-3}.

When it is necessary to provide for the condition $|\tan(\chi/2)| \ll 1$, an interesting situation takes place when both detunings are large:

$$\gamma \ll |\Delta_0| < |\Delta_1|.$$

In this case,

$$\left|\tan\left(\frac{\chi}{2}\right)\right| = \left|\frac{(\Delta_1 - \Delta_0)\gamma_\perp}{\Delta_1 \Delta_0}\right| \ll 1,$$

and the overdamping condition takes the form of inequality

$$\varepsilon = \frac{\Delta_0^2}{\omega_R \gamma} \frac{\Delta k}{k} \ll 1$$

which is well fulfilled in a broad range of parameters provided that $\Delta k/k \ll 1$.

Mathematically, the condition (26) is manifested by the fact that, upon the passage to dimensionless variables

$$\mathbf{r} \longrightarrow \Delta k\mathbf{r}, \quad \mathbf{v} \longrightarrow \mathbf{v}/u_0,$$

$$t \longrightarrow \tau = \Omega^2 t/\kappa, \quad \mathbf{F}_R \longrightarrow \mathbf{u}(\mathbf{r}) = \mathbf{F}_R/m\kappa u_0,$$

(where $\mathbf{v}$ is the particle velocity and $u_0 = F/m\kappa$), the equations of particle motion under the RRF action transform into a system of singular perturbed differential equations

$$\frac{d\mathbf{r}}{d\tau} = \mathbf{v}, \quad \varepsilon\frac{d\mathbf{v}}{d\tau} + \mathbf{v} = \mathbf{u}(\mathbf{r}), \tag{27}$$

where the notations $\mathbf{v}$ and $\mathbf{r}$ are retained for the dimensionless quantities. The methods of investigation of the systems of this type and their reduction to the equations of lower dimensionality are well developed in the theory of differential equations [25, 26]. A solution to the system (27) with arbitrary initial conditions $\{\mathbf{r}_0, \mathbf{v}_0\}$ can be represented in the form of a combination of a rapid transient process described by the boundary functions of the type [25]

$$\Pi\mathbf{v}(\tau) \sim \exp(-\tau/\varepsilon), \quad \Pi\mathbf{r}(\tau) \sim \varepsilon\exp(-\tau/\varepsilon),$$

exponentially decaying within a characteristic time $\tau \sim \varepsilon(t \sim \kappa^{-1})$ and a slow motion over a surface (integral manifold [26]) of the type

$$\mathbf{v} = \mathbf{G}(\mathbf{r}, \varepsilon) \tag{28}$$

in the phase space. In our case, the function $\mathbf{G}$ can be determined using a regular expansion into series with respect to the parameter ε

$$\mathbf{G} = \mathbf{G}_0 + \varepsilon\mathbf{G}_1 + \dots. \tag{29}$$

Substituting this expansion into Eqs. (27), we obtain a sequence of $\mathbf{G}_n$ values

$$\mathbf{G}_0 = \mathbf{u}(\mathbf{r}), \quad \mathbf{G}_1 = -\varepsilon(\mathbf{u}(\mathbf{r})\nabla)\mathbf{u}(\mathbf{r}) \tag{30}$$

and an equation describing the particle trajectory in a light wave field (for $\tau < 1/\varepsilon^2$, expansion (29) can be restricted to the first two terms):

$$\frac{d\mathbf{r}}{d\tau} = \mathbf{u}_1(\mathbf{r}) = \mathbf{u}(\mathbf{r}) - \varepsilon(\mathbf{u}(\mathbf{r})\nabla)\mathbf{u}(\mathbf{r}),$$ (31)

$$\mathbf{r}(0) = \mathbf{r}_0 + O(\varepsilon).$$

According to Eqs. (28) and (31), the stationary velocity of a resonance particle (established by the time $t > \kappa^{-1}$) adiabatically "follows" its spatial position. A relationship between the particle velocity $\mathbf{u}_1(\mathbf{r})$ and the RRF component $\mathbf{F}_R(\mathbf{r})$ has a nonlocal character. The velocity $\mathbf{u}_1$ at each point $\mathbf{r}$ depends both on the force $\mathbf{F}_R(\mathbf{r})$ at this point and on the derivative of $\mathbf{F}_R$ with respect to the spatial coordinates. Therefore, the RRF vector lines in the general case do not coincide with the particle trajectory: $\mathbf{u}_1(\mathbf{r}) \neq \mathbf{u}(\mathbf{r})$. An allowance for the terms on the order of ε in the right-hand part of (31) is important when the RRF vortex component induced by a bichromatic field is dominating, since this very contribution may account for the instability of a rotational particle motion in this case.

The results of numerical calculations of the particle trajectories based on Eqs. (31) showed that the character of motion is highly sensitive with respect to both the spatial configuration and parameters of the light field (frequency detunings). For all configurations, there exists a broad range of these parameters for which the particles may perform finite motions in the cells of effective superlattices.

For the field configuration of the first type described by Eq. (16) (Fig. 1a), the motion is always potential (curl $\mathbf{u}_1(\mathbf{r}) = 0$) and leads for $t \sim t_0 = \kappa/\Omega^2$ to the localization of particles at the sites of a cubic lattice corresponding to the local minima of a potential $U(\mathbf{r})$ determined by Eq. (17).

For the field configuration of the second type (3D$Lin \perp Lin$, Fig. 1b), an analogous potential motion takes place only for specially selected detunings of the field frequencies: $\Delta_1\Delta_0 = -\gamma_\perp^2$ with $|\tan(\chi/2)| \longrightarrow \infty$. In the general case, when this condition is not fulfilled, curl $\mathbf{u}_1(\mathbf{r}) \neq 0$ and the motion exhibits a vortex character. Figure 4 shows a typical particle trajectory for $|\tan(\chi/2)| \sim \varepsilon \ll 1$, representing a helix with nonmonotonically (!) varying radius wound on a nodal line of the RRF vortex component. As was noted in Section 3, the axes of particle rotation (parallel to the field symmetry axis) can be readily controlled by consistently changing the field polarizations.

For the field configuration of the third type described by Eq. (23) (Fig. 1c), the motions along the z axis and in the directions parallel to the xy plane are completely separated and independent. The motion
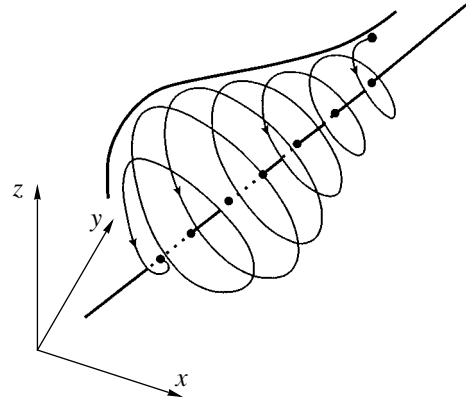

Fig. 4. A trajectory of the light-induced vortex motion (curl $\mathbf{u}_1 \neq 0$) of resonance particles in a field with the 3D$Lin \perp Lin$ configuration.

along the z axis leads eventually to a stable particle grouping in the planes

$$z = (\pi/\delta k)n,$$

where n are the arbitrary integer numbers. The character of the vortex motion of particles in these planes is determined by the ratio of the $\tan(\chi/2)$ and ε. For

$$|\tan(\chi/2)| \lesssim 1/\sqrt{\varepsilon}, \quad \Gamma > 0,$$

the points $\mathbf{r}_m$ (indicated by dots in Figs. 2 and 3) corresponding to minima of the $U(\mathbf{r})$ function (see Eqs. (24)) are stable focuses of the system of differential equations (31) and, hence, the points of localization of the particles forming a regular hexagonal lattice. For

$$|\tan(\chi/2)| \gtrsim 1/\sqrt{\varepsilon}$$

these focuses become unstable, while stable limiting cycles (depicted by dashed lines in Fig. 3) appear inside the triangular regions of the kagome lattice. An explicit form of the parameter ξ for this bifurcation (Hopf bifurcation) can be derived from an analysis of stability of system (31):

$$\xi = |\tan(\chi/2)| - s,$$ (32)

where

$$s = \frac{\kappa}{G}, \quad \kappa \approx -\frac{3\omega_R\Delta_0 g_0\gamma}{|\nu_0|^2},$$

$$G^2 = \omega_R g_0 g_1 3\sqrt{3}|\Gamma\beta|, \quad g_\alpha = \left|\frac{V_\alpha}{\nu_\alpha}\right|^2,$$

$$\tan\left(\frac{\chi}{2}\right) \approx -\frac{\gamma_\perp\Delta_1}{\Delta_1\Delta_0 + \gamma_\perp^2}, \quad \Delta_0 < 0,$$

and the consideration was restricted for simplicity to the most interesting case of

$$|\Delta_0| < \gamma \ll |\Delta_1|, \quad g_0 \sim \left|\frac{V_1^2}{\nu_1 \nu_0}\right| \sim g.$$

The limiting cycles appear for $\xi > 0$; in the case of $0 < \xi/s \ll 1$, these cycles acquire the form of circular trajectories with the radius proportional to $\sqrt{\xi/s}$. The direction of rotation depends on the sign of the angular deviation β. As the sign of Γ changes to opposite, the limiting cycles pass to the neighboring triangular cells. Note that the adjustment to the regime of stable particle rotation depends in a sharp and complicated manner on the field frequency detunings and in a smooth manner, on the geometric factor (angular deviation).

For $|\tan(\chi/2)| \longrightarrow \infty$, when the RRF vortex component fully dominates, the orbits of rotating particles are "pressed" arbitrarily close to the boundaries of separatrix cells. Here, we may introduce small additive fluctuating terms (with a broad frequency spectrum) into the right-hand part of Eqs. (31) so as to model the real quantum fluctuations of the radiative forces [2]. In this case, the particles on the trajectories pressed to the cell boundaries will cross this boundary in the region of saddle points (i.e., the points of intersection of the separatrix lines in Fig. 3) and pass to the boundaries of the adjacent cells. As a result, the particles perform the infinite motion appearing as a random (brownian) walk over edges of the kagome lattice.[5] A similar phenomenon of the light-induced random walk of particles over the edges of effective square lattices in the case of strong fields with a 2D configuration was originally reported in [6].

Finally, let us present some numerical estimates illustrating the possibilities of a mechanical action of light upon atoms in the system studied. For certainty, we will consider resonance particles with $m = 40$ amu exposed to a field of mutually orthogonal standing weaves with $\hbar\omega_0 \approx 3$ eV, $\gamma \approx 3 \times 10^8$ s^{-1}, $\Delta_0 = -\gamma/5$, and $|\Delta_1| = 10^{12}$ s^{-1}. The electromagnetic wave intensities I_α for each frequency component ($\alpha = 0, 1$) were selected so as to satisfy the weak field criterion:

$$g = |V_{j0}/\nu_0|^2 = |V_{j1}^2/\nu_0 \nu_1| = 2 \times 10^{-2},$$

which was achieved for $I_0 \approx 1.5$ mW/cm^2 and $I_1 \approx 10$ W/cm^2 (in this case, $|\rho^{(3)}/\rho^{(1)}| \sim 10^{-1}$). Then, using

Eq. (17) and formulas derived in this section, we obtain the potential

$$\Delta U \approx U_0 \approx 7 \times 10^{-3} \text{ K},$$

the macroscopic lattice period

$$\lambda_M = 2\pi/|\delta k| = 1.8 \text{ mm},$$

and the other quantities:

$$T \approx 10^{-3} \text{ K } ((\Delta U/T) \approx 7), \quad \kappa \sim 10^4 \text{ s}^{-1},$$
$$t_0 \sim (\Omega^2/\kappa)^{-1} \sim 10^{-3} \text{ s} \quad (\varepsilon \sim 0.1),$$
$$F \sim 10^{-5} \text{ eV/cm}.$$

By significantly decreasing detuning of the field $\mathbf{E}_1$ (thus, increasing the macroscopic spatial scale λ_M), it is possible to create a superdeep potential well—a purely optical 3D trap for atoms—using bichromatic laser beams of a large diameter ($b \gtrsim 10$ cm). For example, in the case of $|\Delta_1| = 1.5 \times 10^{10}$ s^{-1} ($\lambda_M \approx 10$ cm), $I_0 \approx 1.5$ mW/cm^2, and $I_1 \approx 150$ mW/cm^2, the potential well depth is $\Delta U = 0.5$ K and $\Delta U/T \sim 500(!)$ for the characteristic time of particle localization $t_0 \approx 0.03$ s. Thus, the right-hand inequality (25) characterizing the efficacy of the RRF action upon the resonance particles, can be satisfied with a large margin under quite realistic conditions.

For the comparison, it is interesting to note that the passage to a "strong field" regime [4]

$$|V_1^2/\gamma\Delta_1| \sim |V_0^2/\gamma\Delta_0| = g_1 \gg 1, \quad |\Delta_0| \gg \gamma,$$

for the same level of saturation ($|V_0^2/\Delta_0^2| = g$) and detuning $|\Delta_1|$ as in the example given above, the field intensities E_0 and E_1 must be increased by a factor of g_1^2/g and g_1/g, respectively. As a result, the RRF magnitude and the potential ΔU will increase only by a factor of g_1 ($g_1 \ll g_1^2/g$, g_1/g) and the $\Delta U/T$ ratio will remain unchanged (because $T \sim \hbar\gamma g_1 \gg \hbar\gamma$ [14]).

5. CONCLUSION

Under the physical conditions studied, the system is always characterized by a small degree of occupation of the atomic states ($\rho_{ii} \ll 1$) and by small values of the light-induced Stark shift (the latter circumstance is important for the spectroscopic applications). Nevertheless, the RRFs can be sufficiently large to effectively act upon an atomic ensemble with a temperature corresponding to the Doppler cooling limit.

Based on an analysis of the general relationships derived for the RRFs, we found symmetric configurations of the interfering waves for which the spatial structure of the light-induced force field can be effectively controlled by consistently changing the frequencies of the optical fields, which allows the ratio of the

---

[5] It is interesting to note that, according to the results of numerical calculations, the walk over boundaries of the separatrix cells is also observed in the absence of small fluctuating forces, provided that the calculation time is sufficiently large, which is probably related to the "noise" introduced by the so-called discretization errors. The time of a particle escape from the cell may depend on the numerical method selected. Similar discretization effects, arising during a dynamic chaos simulation in the Hamiltonian systems, are considered, for example, in monograph [27].

vortex and potential RRF components to be varied almost arbitrarily.

It was found for the field configurations studied that it is possible to remove, in a broad range of the control parameters, some fundamental limitations of the type of the Earnshaw optical theorem (proved for weak monochromatic fields [23], see also [5, 6]) prohibiting the 3D localization (confinement) of the resonance particles by means of the spontaneous light-induced pressure. The light-induced motion of a confined resonance particle proceeds inside an elementary cell of an effective optical superlattice (with a cubic or hexagonal structure for the field configurations studied). This motion is finite and exhibits a vortex or potential character, depending on the frequency detunings selected, and leads eventually to the localization (confinement) of particles at the RRF nodes or to their stable rotation along closed orbits inside the elementary lattice cells. The transition from a light-induced potential motion to the vortex motion and a change of the axes of particle rotation during the vortex motion can be also provided by consistently varying polarizations of the interfering waves without altering their propagation directions. A polarization effect of this type is manifested in a field configuration of the 3D$Lin \perp Lin$ type.

In a situation of the absolutely dominating vortex RRF component, a very interesting regime of the light-induced infinite motion of particles is possible in the form of their random walk over edges of a planar superlattice of the kagome type (for the field configuration depicted in Fig. 1c).

The rectified radiative forces can be used for controlling the motion of resonance particles, creating stable periodic 3D structures in a cold atomic gas, and constructing purely optical (nonmagnetic) macroscopic traps (using laser beams of large diameter) capable of trapping large-size bunches of resonance particles. An example of interesting application is offered by the purely optical confinement of an ultracold rarefied plasma bunch with resonance ions [19, 28, 29].

ACKNOWLEDGMENTS

REFERENCES

1. A. P. Kazantsev, G. I. Surdutovich, and V. P. Yakovlev, *The Mechanical Action of Light on Atoms* (Nauka, Moscow, 1991).

2. V. G. Minogin and V. S. Letokhov, *The Pressure of Laser Radiation on Atoms* (Nauka, Moscow, 1986).

3. V. S. Letokhov, M. A. Ol'shanii, and Yu. B. Ovchinnikov, Quantum Semiclassic. Opt. **7**, 5 (1995).

4. A. P. Kazantsev and I. V. Krasnov, Pis'ma Zh. Éksp. Teor. Fiz. **46**, 264 (1987) [JETP Lett. **46**, 332 (1987)].

5. A. P. Kazantsev and I. V. Krasnov, Zh. Éksp. Teor. Fiz. **95**, 103 (1989) [Sov. Phys. JETP **68**, 59 (1989)].

6. A. P. Kazantsev and I. V. Krasnov, J. Opt. Soc. Am. B **6**, 2140 (1989).

7. A. P. Kazantsev and I. V. Krasnov, Phys. Lett. A **127**, 33 (1988).

8. R. Grimm, Yu. B. Ovchinnikov, A. I. Sidorov, and V. S. Letokhov, Phys. Rev. Lett. **65**, 1415 (1990).

9. V. S. Voĭtsekhovich, M. V. Danileĭko, A. M. Negriĭko, *et al.*, Zh. Éksp. Teor. Fiz. **99**, 393 (1991) [Sov. Phys. JETP **72**, 219 (1991)].

10. J. Juvanainen, Phys. Rev. Lett. **4**, 519 (1990).

11. R. Grimm, J. Soding, and Yu. B. Ovchinnikov, Pis'ma Zh. Éksp. Teor. Fiz. **61**, 362 (1995) [JETP Lett. **61**, 367 (1995)].

12. J. Soding, R. Grimm, Yu. B. Ovchinnikov, *et al.*, Phys. Rev. Lett. **78**, 1420 (1997).

13. T. T. Grove, B. C. Duncan, V. Sanchez-Villicana, *et al.*, Phys. Rev. A **51**, R4325 (1995).

14. I. V. Krasnov, Laser Phys. **4**, 906 (1994).

15. I. V. Krasnov, Zh. Éksp. Teor. Fiz. **107**, 1135 (1995) [JETP **80**, 632 (1995)].

16. H. Pu, T. Cai, N. P. Bigelow, *et al.*, Opt. Commun. **118**, 261 (1995).

17. E. A. Korsunsky and D. V. Kosachiov, J. Phys. B **30**, 5701 (1997).

18. G. Wasik and R. Grimm, Opt. Commun. **137**, 406 (1997).

19. A. P. Gavrilyuk, I. V. Krasnov, and N. Ya. Shaparev, Pis'ma Zh. Éksp. Teor. Fiz. **63**, 316 (1996) [JETP Lett. **63**, 324 (1996)].

20. A. P. Gavrilyuk, I. V. Krasnov, S. P. Polyutov, and N. Ya. Shaparev, Vychisl. Tekhnol. **4**, 43 (1999).

21. A. Hemmerich and T. W. Hansh, Phys. Rev. Lett. **68**, 1492 (1992).

22. T. Walker, P. Feng, D. Hoffmann, and R. S. Williamson, Phys. Rev. Lett. **69**, 2168 (1992).

23. A. Ashkin and J. P. Gordon, Opt. Lett. **8**, 511 (1983).

24. A. P. Kazantsev, V. S. Smirnov, G. I. Surdutovich, *et al.*, J. Opt. Soc. Am. **2**, 1731 (1985).

25. A. B. Vasil'eva and V. F. Butuzov, *Asymptotic Expansions of Singular-Perturbed Equations* (Nauka, Moscow, 1973).

26. Yu. A. Mitropol'skiĭ and O. B. Lykova, *Integral Manifolds in Nonlinear Mechanics* (Nauka, Moscow, 1973).

27. G. M. Zaslavskiĭ, V. Z. Sagdeev, D. A. Usikov, and A. A. Chernikov, *Weak Chaos and Quasi-Regular Structures* (Nauka, Moscow, 1991).

28. A. P. Gavrilyuk, I. V. Krasnov, and N. Ya. Shaparev, Laser Phys. **8**, 653 (1998).

29. S. A. Gavrilyuk, I. V. Krasnov, S. P. Polyutov, and N. Ya. Shaparev, in *Proceedings of 5th Russian-Chinese Symposium on Laser Physics and Technologies* (Tomsk State Univ., Tomsk, 2000).

Translated by P. Pozdeev